Phantom and clinical evaluation of Block Sequential Regularized Expectation Maximization (BSREM) Reconstruction Algorithm in 68Ga-PSMA PET/CT Studies

Fatemeh Sadeghi
Tehran University of Medical Sciences
Peyman Sheikhzadeh (psh82@yahoo.com)
Tehran University of Medical Sciences https://orcid.org/0000-0003-3053-2641
Nima Kasraie
UT Southwestern: The University of Texas Southwestern Medical Center
Saeed Farzanehfar
Tehran University of Medical Sciences
Mehrshad Abbasi
Tehran University of Medical Sciences
Yalda Salehi
Tehran University of Medical Sciences
Mohammad Reza Ay
Tehran University of Medical Sciences

Research Article

Keywords: Image Reconstruction, PET-CT Scan, Prostate Cancer, Bayesian Approach

Posted Date: December 15th, 2022

DOI: https://doi.org/10.21203/rs.3.rs-2334561/v1

Abstract

Purpose

we aimed to investigate the effect of various β-value in BSREM algorithm under different lesion sizes, in order to determine an optimal penalty factor for clinical use.

Methods

The NEMA IQ phantom and 15 patients with prostate cancer were injected with 68Ga-PSMA and scanned by GE Discovery IQ PET/CT scanner. Images were reconstructed using OSEM and BSREM with different β-values and then background variability (BV), contrast recovery (CR), signal-to-noise ratio (SNR), and lung residual error (LE) from phantom data, and Signal-to-Background Ratio (SBR), contrast from clinical data were measured.

Results

The increment of BV using β-value of 100 was 120% and the decrement of BV using β-value 1000 were 40.5% compared to OSEM. As the β decreased from 1000 to 100, the SUV_{max} increased by 59% and 26.4% for sphere with diameter of 10 mm and 37 mm, respectively.Δ $SNR_{(100\text{-}1000)}$ % increased by 140.5 and 29.0 in the smallest and the largest sphere, respectively. The Δ LE $_{OSEM\text{-}100}$ and Δ LE $_{OSEM\text{-}1000}$ was − 41.1% and − 36.7% respectively. In the clinical study, the lowest SBR and contrast was related to the OSEM. The SBR and contrast, respectively increased by 69.7% and 71.8% in small lesions and 35.6% and 33% in large lesions, respectively, when β-value was decreased from 500 to 100.

Conclusions

As the lesion size decreased, the optimum β-value decreased. In both studies, a β value of 400 would be optimal for reconstruction of small lesions, whereas for large lesions in phantom and clinical studies respectively, β-value of 600 and 500 is recommended.

Introduction

PET-CT today is one of the standard of care imaging options in oncology diagnosis as well as for assesment of response to treatment [1]. The choice of the image reconstruction algorithm has great impact on the accuracy and reproducibility of quantitative measurments in PET imaging [2]. Iterative reconstruction methods such as Ordered Subset Expectation Maximization (OSEM) provide more improvement in overall image quality and SNR compared to previously used analytic methods. However, OSEM reconstruction has a serious limitation, namely, the image noise is adversely tied to the iteration

number so that image noise intensifies with the increase in the number of iterations, limiting the ability to detect small lesions [3]. An earlier terminating iteration (usually 2 or 4) and post-filtering assist to reduce image noise, although incomplete convergence and inaccuracy of quantification will result as a consequence of lower iterations including underestimation of smaller lesion SUVs[4].

With the continued advancement of iterative reconstruction methods, recently a novel block sequential regularized expectation maximization (BSREM) algorithm has been developed [5]. BSREM uses point speared function modeling (PSF) and a penalty term that allows for high iteration without the consequential image quality degradation [6]. The global smoothing parameter β is adjustable by the user and enables one to monitor the trade-off between spatial resolution and image noise. Thus β acts as a penalization factor that suppresses excessive image noise in high iteration numbers, where full convergence of each voxel can lead to improve accuracy of quantitative measurments such as pricise SUV in smaller lesions.

In nuclear medicine, a wide array of radiopharmaceuticals according to their characteristics for specific diseases are used. The parameter β is positrone range dependent. Therefore extensive studies for each radiopharmaceutical are needed to determine the performance of BSREM reconstruction algorithm on image qualifications as well as image quantification. Previous studies have extensively investigated the efficacy of BSREM on 18F-FDG PET imaging as the most widely used radiopharmaceutical in the diagnosis of cancers. For example, Liberini et al. investigated the BSREM using β-value of 450 in 18F-FDG PET-CT scans of patients with in-transit metastases of malignant melanoma. Their results showed more lesion detectability, higher SUV_{max}, and better target to background ratio in BSREM compared to OSEM (39%, 76.5% and 77% respectively) [7]. Caribe et al also performed phantom and clinical scans with the aim of BSREM evaluation in 18F-FDG PET-CT examinations, and as per other studies, found that BSREM led to higher CR and contrast-to-noise ratio (CNR) with concurrent lower noise [8]. In our study, we analysed the performance of BSREM in 68Ga-PSMA PET-CT imaging. 68Ga has a distinct distribution pattern from other tracers, and its use for prostate cancer diagnosis has been a significant recent advancement in nuclear medicine imaging [9]. Certain small sized subcentimetric pelvic lymphnodes are involved by the tumor and understimation of the SUV_{max} results in false negative reports. Many previous studies have examined the improvement of BSREM in 68Ga-PSMA imaging on PET scanners with LYSO crystals using time-of-flight (TOF) technology. To our knowledge, however, it has not been assessed in terms of lesion size. For example, Jonmarker et al,. studied 61 patients with prostate cancer that were scanned on a GE Discovery MI scanner with LYSO crystals. Images were reconstructed with OSEM and BSREM using β-value of 700 (both algorithms consist of TOF and PSF techniques). They concluded that BSREM found fewer ambiguous lesions compared to OSEM (175 and 187 lesions in BSREM and OSEM respectively) [10]. Lindström et al analysed data of patients with recurring prostate cancer and also scanned them with a GE Discovery MI and reconstructed images with TOF OSEM vs TOF BPL with β-values of 100–1300 at intervals of 100. The noise of images using the OSEM method was 15%, while the noise was remarkably lower in BSREM images with β-values exceeding 300 (36% in $BSREM_{100}$ and 8% in $BSREM_{1300}$) and the SNR increased by 25% and 66% in $BSREM_{200}$ and 1300

compared to OSEM respectively [11]. Data acquisition in our study was performed using the injection of 68Ga-PSMA and a non-TOF PET-CT scanner with BGO crystals. Furthermore, we investigated the impact of lesion size on the results of BSREM algothim.

The aim of this study was therefore to investigate the effect of various strengths of noise penalization factor in 68Ga-PSMA imaging with a BGO scanner for clinical use in patients with prostate cancer. In order to determine an optimum penalty factor by considering both quantitative and qualitative image evaluation parameters, we analyzed both phantom and clinical data under various lesion sizes.

Methods

A. PET-CT System and Reconstruction Algorithm

All data were acquired using a digital GE Discovery IQ PET-CT scanner (GE Healthcare, Waukesha, WI, USA) with a 5-ring setup installed at nuclear medicine department of a university hospital, Tehran University of Medical sciences.. This non-TOF scanner has bismuth germanium oxide (BGO) detectors. Each ring with a diameter of 74 cm consists of 36 detector blocks which provide a trans-axial and axial field of view (FOV) equal to 70 cm and 26 cm respectively. The scanner has 79 image planes, 3.27-mm plane spacing and bed overlap ranges from 10–24%. Its coincidence window is 9.5nsec with 720 photomultipliers in total. For the purpose of attenuation and scatter correction, a 16-slice CT scanner with full rotation degree acompanies the PET system [12]. The aqcuired raw data were reconstructed by using OSEM methodology with 4 iterations, 24 subsets and was post processed with 4.8 mm Gaussian filter. Likewise, BSREM with 25 iterations, with no post filtering but using β-value from 100 to 500 for clinical data and from 100 to 1000 for phantom data at an interval of 100 was applied.

B. Phantom Study

A set of National Electrical Manufacturers Association (NEMA) image quality phantom (NEMA Standards Publication No. NU2, National Electrical Manufacturers Association, Washington, DC, 2001) was assessed in this study. The NEMA phantom with volume of 9780 ml has 6 fillable spheres with different inner diameters of 10 mm, 13 mm, 17 mm, 22 mm, 28 mm and 37 mm, and a lung insert with diameter of 44.5 mm is also positioned inside it [13]. We filled the background volume of phantom with 5 kBq/ml of 68Ga-PSMA radiopharmaceutical. The spheres were filled with lesion to background ratio of 4 (LBR = 4:1) to simulate the uptake of clinical tumors. In addition, to further simulate the human lung tissue, we filled the lung insert with water and Styrofoam. For imaging, the phantom was located in the center of the FOV and scanned according to the NEMA procedures [14]. All phantom scans with various β-values were obtained using a 2 min acquisition duration per each bed position.

We analyzed the data following the NEMA analysis tool to measure the background variability (BV), and the quantitative features in spheres $\mathrm{namelythe}SUV_{max}$, contrast recovery (CR), signal to noise ratio (SNR), and lung residual error (LE) in the lung insert [15]. To calculate the BV, we drew a total of 60

regions of interest (ROIs) with 5mm diameter, on the background of 5 central slices of spheres (each slice consisting of 12 ROIs). BV was calculated as standard deviation (SD) of the background ROI counts divided by the average background ROI counts. To include spheres, we placed volume of interest (VOI) with the individual diameter according to sphere diameter in the central slice of spheres. The CR of each sphere size was calculated as [16]:

$$CR=\frac{\frac{C_H}{C_B}-1}{\frac{a_H}{a_B}-1} \quad (1)$$

where C_H and C_B are mean counts of each VOI and mean counts of 60 ROIs in the background respectively. $\frac{a_H}{a_B}$ is the ratio of activity in hot lesions to background that is equal to Lesion-to-Background Ratio (LBR). The measurement of SNR was defined as mean voxel count of each VOI divided by the SD of the activity of background ROIs. The LE was calculated as the ratio of mean activity in lung insert to mean activity in background ROIs.

C. Clinical Study

Clinical data from 3-dimensional whole-body 68Ga-PSMA PET-CT of 15 patients were analyzed in this research study. Patients with prostate cancer and metastases of different sizes in the whole body were retrospectively selected who had been scanned from September 2021 through February 2022. The patients had weight ranging from 55 to 98 kg, with average hight of 168 cm and the average age of 68 ± 9.5 years. Patients were intravenously injected based on recomneded activity for 68Ga-PSMA which is 1.85 MBq per kilogram of body weight (0.05 mCi/kg) for clinical use and data aqcusition started almost 60 min after injection. Patients were scanned from vertex to mid-thigh, and all clinical scans were obtained using a 3 min acquisition duration for each bed position.

For assessing the images, we placed VOI around the lesions to encompass them. In total we found 50 lesions in the 15 patients that were classified into 3 size groups: lesions with diameter ≤ 10 mm (n = 15), lesions with diameter between 10 and 20 mm (n = 20), and lesions with diameter ≥ 20mm (n = 15). We analyzed clinical data in terms of image noise, SUV_{max}, SNR, signal to background ratio (SBR) and contrast. For calculating image noise, in the largest slice of the right lobe of the liver and a slice before and after it, we placed 9 ROIs with diameter of 3mm in the homogenous area of the liver (each slice consisting of 3 ROIs and avoiding vessels and portal vein). The noise in the clinical data was defined as the ratio of SD to the mean activity of 9 ROIs in the liver (similar to the equatation of BV in the phantom data). The SNR of each lesion was measured as the individual lesion SUV_{max} devided by noise. We located one ROI with a diameter of 10mm in the homogenous area of the liver as a liver reference. The SBR we defined as [16]:

$$SBR=\frac{SUV_{max}lesion}{SUV_{mean}reference}\times 100 \quad (2)$$

The contrast was measured as the ratio of maximum activity of lesion to mean activity of the 9 ROIs in the liver.

D. Statistical analysis

To evaluate the results of BSREM reconstructions with OSEM or differences between the results of two β-values, we used a paired sample t-test with p-value < 0.05 as statistically significant. furthermore, we used ANOVA analysis to assess the significant differences between multiple reconstructions. In this research, all the statistical analyses were done with SPSS release 23.0 (IBM Corporation, Armonk, NY, USA).

To make a comparison for the effect of different β-values, we compared the relative increase or decrease of each evaluation parameter at an equal interval of β-value. For these purposes, the relative difference of evaluation features from old reconstruction (a) to new reconstruction (b) were calculated as:

$$\Delta feature_{(a-b)}\% = \frac{feature_b - feature_a}{feature_a} * 100 \quad (3)$$

Results

A. NEMA Phantom

The results of SUV_{max} in different lesion sizes and BV are shown in Fig. 1. The BV decreased with increasing β-value. There was not a consistent increase in BV by reducing β-value, but the BV variation rather flattened above $BSREM_{700}$: As the β increased from 700 to 800, from 800 to 900, and from 900 to 1000, the BV decreased by 5.5%, 4.6% and 3.9% respectively. The increase of BV using β-value of 100 was 120% and the decrease of BV using β-value of 500 and 1000 were 3.9% and 40.5% compared to OSEM respectively. All plots of SUV_{max} in different lesion sizes in BSREM reconstruction show a similar trend, so the SUV_{max} increased with decreasing β-value. As the β decreased from 1000 to 100, the SUV_{max} increased by 59%, 27.1% and 26.4% for the smallest sphere(37mm), sphere with diameter of 22mm and the largest sphere respectively. There is not a significant difference on SUV_{max} behaviour in higher β-values. The SUV_{max} using $BSREM_{800}$, $BSREM_{900}$ and $BSREM_{1000}$ were 4.83, 4.75, 4.69 for the smallest sphere, 10.9, 10.5 and 10.1 for the 22mm sphere, and 15.8, 15.75 and 15.7 in the large sphere with diameter 37mm.

In Fig. 2, the central slice of phantom data were shown for $BSREM_{100-1000}$ and OSEM. The Figure illustrates insufficient noise supression in BSREM using lower β-value and higher BV which are undesirable for clinical purposes degrading image quality. On the other hand the potential of high β-values in smoothing background and enhancement contrast translated into an improvement in lesion detectibility and overall image quality.

The relative differences of CR in various sphere diameters were summarized in Table 1. For all sphere sizes, there was a negetive correlation between β-value and CR. Hence as the β-value increases, the CR decreases such that the highest CR was attributable to BSREM with β-value of 100. The relative difference of CR by increasing β-value from 100 to 1000 ($\Delta CR_{100-1000}$) was − 61.7%, -23.2% and − 11.2% in spheres with diameter of 10mm, 22mm and 37mm respectively. In the smallest sphere (10mm), β-values equal or exceed 500 created lower CR than OSEM, whereas in the largest sphere (37mm), the CR of BSREM was higher than CR of OSEM, irrespective of β-value. The $\Delta CR_{OSEM-100}$, $\Delta CR_{OSEM-500}$, $\Delta CR_{OSEM-1000}$ respectively was 80.3%, -1.9% and − 3.2% in smallest sphere (10mm) and 22.7%, 7.4% and 0.2% in sphere with diameter of 22mm, and 12.9%, 5.2% and 5.9% in the largest sphere (37mm).

Table 1
The relative difference of CR for hot spheres with diamater of 10 mm, 13 mm, 17 mm, 22 mm, 28 mm and 37 mm in NEMA image quality phantom study. Images were reconstructed by BSREM using β-value in a range between 100 and 1000 and OSEM algorithm. *P*-values from student t-test between two reconstruction methods are mentioned.

	Lesion size(mm)						**t-test**
Relative difference of CR	10	13	17	22	28	37	p^*
$\Delta CR_{(200-100)}\%$	24.48	13.58	6.08	3.86	2.77	1.96	$<10^{-4}$
$\Delta CR_{(300-200)}\%$	17.47	12.11	5.65	3.44	2.36	1.67	$<10^{-6}$
$\Delta CR_{(400-300)}\%$	13.41	11.48	5.5	3.25	2.19	1.47	$<10^{-5}$
$\Delta CR_{(500-400)}\%$	10.86	10.33	5.2	3.02	2.01	1.33	$<10^{-4}$
$\Delta CR_{(600-500)}\%$	8.85	9.17	4.93	2.86	1.91	1.27	$<10^{-6}$
$\Delta CR_{(700-600)}\%$	8.03	8.54	4.73	2.73	1.78	1.15	$<10^{-5}$
$\Delta CR_{(800-700)}\%$	7.17	7.82	4.53	2.63	1.7	1.09	$<10^{-4}$
$\Delta CR_{(900-800)}\%$	6.51	7.2	4.34	2.54	1.64	1.04	$<10^{-5}$
$\Delta CR_{(1000-900)}\%$	5.98	6.66	4.17	2.46	1.59	1.006	$<10^{-5}$
$\Delta CR_{(1000-100)}\%$	161.6	128.83	55.36	30.25	19.49	12.66	$<10^{-4}$
$\Delta CR_{(OSEM-100)}\%$	80.35	76.56	38.84	22.72	18.79	12.93	$<10^{-5}$
$\Delta CR_{(OSEM-1000)}\%$	-31.05	-22.84	-10.63	-5.77	-0.59	0.23	$<10^{-4}$

Figure 3 shows the SNR of 3 hot spheres (10mm, 22mm and 37mm) that were reconstructed using different algorithms. The results of SNR demonstrated an increase in β-value translated into an increase in SNR, while the lower β-values (100 and 200) had insufficient SNR due to their excessive noise levels. The SNR of $BSREM_{100}$ was 12.02, 52.8, 83.8 in spheres with diameter of 10mm, 22mm and 37mm respectively, while the SNR of OSEM reconstruction in these sphere sizes was 22.2, 70.8 and 100.2. The relative differences of SNR was dependent on sphere size. As the β-value increased from 100 to 1000, the SNR also increased by 140.5%, 37.6% and 29% in the smallest, mid and largest spheres respectively. Using $BSREM_{500}$ and above resulted in higher SNR compared to OSEM, except for the biggest sphere. In the largest sphere, only β-value of 100 and 200 had lower SNR than OSEM. The Δ $SNR_{OSEM-700}$ was 19.9% and 6.7% in the smallest and largest spheres respectively. The calculated LE from BSREM reconstruction showed various β-values resulted in almost similar LE, so that the maximum relative difference of LE between various β-values was 12.9%. BSREM using all examined β-values, resulted into lower LE than OSEM. The Δ $LE_{OSEM-100}$ and Δ $LE_{OSEM-1000}$ was − 41.1% and − 36.7% respectively.

B. Clinical Study

A total of 15 patients with 47 lesions (27 small lesions and 20 large lesions), reffered for the staging of prostate cancer with 68Ga-PSMA PET/CT, were enrolled. Figure 4 demonstrates coronal slices of a sample patient that was reconstructed with BSREM using different β-values and OSEM. Arrows indicate focal 68Ga-PSMA uptake and for each reconstruction, the noise level is mentioned. In Fig. 4, a positive trend can be seen between β-value and image quality. Lower β-values (100–200) suffer from high noise level, while enabling enhancement of lesion uptake. Higher β-values (400–500) provide appropriate lesion conspicuity and image homogeneity so that the detection of small lesions can be as good as finding large lesions.

The results of clinical assessments including SUV_{max}, SNR, SBR, contrast and noise for two lesion sizes and in various reconstruction datasets are shown in the Fig. 5. BSREM using β-values less than 400 leads to an increased noise compared to OSEM. The relative difference of noise by changing reconstruction from OSEM to β-value of 100, 200, 300 was 123.2%, 51% and 15.9% respectively. BSREM using β-value of 500, as the lowest noise reconstruction, had 12.4% less noise than OSEM. As the noise penalization factor (β) increased, SUV_{max} of all lesions decreased. Decreasing β-value from 500 to 100 leads to an increasing SUV_{max} by 73.2% and 37.4% in small and large lesion size groups, respectively. The mean SUV_{max} of small and large lesion size groups for $BSREM_{500}$ was 12.1 ± 2.4 and 25.07 ± 8.1 and the mean SUV_{max} for OSEM was 7.9 ± 3.2 and 21.8 ± 8.6, respectively. The SBR and contrast increase with decreasing β-value, whereas an increase on β-value translates into an increase in SNR. The lowest SBR and contrast was related to the OSEM, irrespective of lesion size and β-value. The Δ $SBR_{OSEM-100}$% and Δ$SBR_{OSEM-500}$%, respectively was 159.9 and 53.1 for small lesions and 54.3 and 13.8 for large lesions, respectively. The same results were seen in contrast so that the Δ $contrast_{OSEM-100}$% and Δ$contrast_{OSEM-500}$% was 169.3 and 56.7 for small lesions and 55.6 and 16.3 for large lesions, respectively. In BSREM algorithm, the relative difference of SBR and contrast was more affected by lesion size; as the lesion size decreased, the relative difference of SBR and contrast

increased. The SBR and contrast, respectively increased by 69.7% and 71.8% in small lesions and 35.6% and 33% in large lesions, when β-value decreased from 500 to 100. In more than 78% of small lesions, the lowest SNR was attributed to OSEM, while in all large lesions, the lowest SNR was attributed to BSREM using β-value of 100. The average of $\Delta\, SNR_{OSEM-100}$% was 17.2 and − 33.6 in small and large lesions, respectively. In the latter, β-values exceeding 200 resulted in higher SNR compared to OSEM. The mean incresse of SNR for large lesions in β-value of 400 and 500 was 32.4% and 53.2% and for small lesions was 82% and 94.6% compared to OSEM, respectively.

Discussion

The relatively new reconstruction algorithm which uses a penalization factor has been widely investigated on TOF LYSO PET/CT scanners using 18-F-FDG but not as much on non-TOF BGO PET/CT systems particularly for 68Ga-PSMA with focus on small sizeed lesions. This study assessed optimal regularization parameter β in the BSREM algorithm, comparing the results with the OSEM counterpart. For this purpose, we performed comprehensive quantitative evaluations on a NEMA phantom with LBR 4:1 and patients with prostate cancer who had underwent 68Ga-PSMA injections for PET/CT imaging.

The potential of BSREM reconstruction in suppression of excessive noise, provides the possibility of using high iterations (about 25 iterations for BSREM compared with conventional OSEM with 4 iterations) in a feasible way. In BSREM, the exceeding noise level is dampened by using a penalization factor [10]. Our phantom assessments revealed that decreasing β-value provided higher SUV_{max}, but at the cost of higher BV, which is not desired in oncological studies (Fig. 1). The comparison of BSREM and OSEM in regards to BV shows that BSREM with β-values above 400 results in lower BV compared to OSEM. At the extreme, disregarding *SUVmax* and using $BSREM_{1000}$ yields images with BV of 4.2, quite lower than OSEM with the corresponding BV at 5.9 (Fig. 1), further corroborating this point.

The results of the clinical part of this study were also in line with our phantom conclusions. As already mentioned, the impact of β-values on image noise has been highlighted in multiple studies in the literature. Liberini et al. analyzed the use of different β-values (100–700, in steps of 100) for detection of brain metastases in 40 patients with lung cancer using 18F-FDG injection. They reported that the accuracy of a $BSREM_{100}$ setting was lower, due to the degradation of image quality by noise [17]. In both our phantom and clinical data, the noise of $BSREM_{400}$ was almost equivalent to that of OSEM reconstruction. This result is also evidenced in another study by Lindström *et al.* where they assessed a NEMA phantom that was filled with 68Ga-DOTATOC with LBR 4.3:1 and 4:1. BSREM with β-values of 133, 267, 400, and 533 and OSEM were used for image reconstruction. Their results revealed $BSREM_{400}$ capable of producing equivalent noise levels to that of OSEM [18].

The elevated number of iterations in BSREM allows each image voxel to reach full convergence, avoiding insufficient iteration problems that can arise from the partial convergence of every single image voxel. Namely, the full convergence translates into improved quantification accuracy of focal uptakes which can be pivotal in clinical diagnosis. For almost all lesion sizes in our phantom study, we reported higher

SUV_{max} in BSREM with β-values less than 700 and lower SUV_{max} with β-values more than 700, when comparing to OSEM. In our clinical study, all BSREM reconstructions led to higher SUV_{max} compared to OSEM, for both small and large lesion size groups (Fig. 5). The relative difference of SUV_{max} looking at OSEM vs. $BSREM_{100}$was 164% and 57.6% in small and large lesion size groups, respectively (Fig. 5). Voert et al investigated 25 patients who underwent 68Ga-PSMA PET/MR and the TOF images were reconstructed with OSEM and BSREM using β-values of 150–1200. They reported that in lesions with low activity, BSREM using β-values higher than 600 led to a lower SUV_{max} than OSEM [19]. The results of Lohaus et al in detection of pulmonary nodules with 18-F-FDG PET/CT showed that the SUV_{max} of nodules was significantly higher in BSREM compared to OSEM (the mean $SUV_{max}$of nodules in $BSREM_{450}$ and OSEM was 5.4 and 3.6, respectively) [20].

In the present study, we show that the BSREM outperformed OSEM at a matched level of noise (Figs. 1 and 5). In the phantom study, the SUV_{max}, CR, SNR of spheres for BSREM were higher or at least similar to those by OSEM. The relative difference of SUV_{max}, CR and SNR for the largest sphere (37mm) from OSEM to $BSREM_{400}$ was 1.1%, 7.3% and 6%, respectively (Figs. 1 and 3, and Table 1). A similar trend in clinical study was observed. For the patient data, at similar noise level, the mean SUV_{max}, SNR, SBR and contrast of lesions were 38%, 49.3%, 36.5% and 40.9% higher than OSEM (Fig. 5). Caribé et al. have similarly shown BSREM to have superior tumor SUV_{mean}, SUV_{max} and contrast compared to OSEM, at the equivalent noise level [8].

The quantitative features of our PET images seem to reach steady values with minimal change when we used BSREM with high β-values. For lower βs at or below 200 however, we observed a high increase in SUV_{max}, BV and CR when decreasing β-value (the $\Delta\ SUV_{max\,(200-100)}$ and the $\Delta\ CR_{(200-100)}$ for lesion size of 10mm being 17.8% and 24.4%, respectively), whereas a negligible gain in quantitative parameters were seen when decreasing β-value from 1000 to 900 (Fig. 1, Table 1, The $\Delta\ SUV_{max\,(1000-900)}$ and the $\Delta\ CR_{(1000-900)}$ for lesion size of 10mm being 1.3% and 5.9%, respectively). Trägårdh et al evaluated BSREM reconstructions in 25 patients who were referred for 18F-FDG imaging using a silicon photomultiplier PET-CT scanner. They used BSREM with β-value of 100-700 for image reconstruction, and found that the lesion SUV_{max}varied considerably in BSREM reconstruction, when they used lower β values [21].

Looking closer at different lesion sizes in our assesment, it can be concluded that BSREM has a greater impact on smaller lesion sizes. This is very crutial for detection of abnormal small size pelvic lymphadenopaties. In the phantom study, the relative difference of lesion uptake and CR from β-values of 1000 to 100 increased by 59–161% for the smallest sphere (10mm) and 26.4–12.6% for the largest sphere (37mm), respectively (Table 1). Also, the $\Delta SNR_{1000-100}$ decreased by 58.4% and 20.5% for the smallest and the largest sphere, respectively. The results of clinical study with different lesion size groups confirmed these results. The lesions with smaller diameter were more affected by the changing β-value, as per Fig. 3. The percentage difference of SUV_{max}, SBR and contrast in BSREM with β-value from 500 to 100 was 73.2%, 69.7% and 71.8% for small lesions and 37.4%, 35.6% and 33% for large lesions (Fig. 5).

The findings of Lindström et al.'s research were thus consistent with our results. They revealed that with increasing lesion volume, the relative difference of SUV_{max} decreased, when comparing BSREM with OSEM. Also they reported no significant difference in SUV_{max} for lesions with volume greater than 3 mL, when increasing lesion size [18]. Wang et al reported showed lesions smaller than 2cm were significantly different in the terms of SUV_{mean}, SUV_{max} and SBR in BSREM with β-value of 570 compared to OSEM, while lesions larger than or equal to 2cm were not affected by these reconstructions [22].

The effect of a low penalizing parameter (β-value ≤ 300) on increasing noise can result in false positive enhancement of lesion uptake estimation or false positive detection of noise instead of lesions. On the other hand, excessive smoothing in BSREM using higher β-values (β-value ≥ 700) may lead to lower SUV_{max} compared to OSEM and consequent false negative rinterpretations. So in general, based on our phantom results, a BSREM technique using β-values in the range between 400 and 600 are recommended for image evaluations, where accurate SUV and more contrast recovery with preserving image quality was obtained. Our clinical assessments supported the aforementioned conclusion: For clinical examinations with 68Ga-PSMA, BSREM using β-values in the range between 400 and 500 seems to be the recommended value for optimum reconstruction. Thus from both a phantom and clinical perspective, for small lesions with low activity, BSREM using β-value of 400 could be an appropriate reconstruction, which increases lesion uptake and contrast as well as maintaining appropriate image noise that could increase the detectability of small lesions. Due to the high acitity in large lesions, there is no requirement to enhance their absorption with applying low β-values. Therefore, in phantom and clinical studies respectively, β-value of 500 and 600 could be optimal for reconstruction for large lesions, with the aim of improving SNR and image conspicuity. This finding is comparable with Voert et al’s result indicating likewise concluded optimal sweetspot for β-values in the range between 400 to 550 by BSREM reconstruction [19].

Our choice of a non-TOF study and the relevant BGO vs LSO based system also necessitates a brief mention. The coincidence window that can be used with BGO systems has to be relatively wider also due to higher sensitivity works with lower activity, hence cannot generally benefit from TOF reconstruction mode. Thus although LSO/LYSO detectors nowadays remain the preferred choice in commercial TOF systems owing to their higher light-yield and faster decay times, BGO scanners do maintain certain advantages and need reconstruction enhancment procedures, namely a higher effective atomic number (ergo increased detection efficiency at 511 keV), lower intrinsic radiation, and lower production costs [23].

In our study, patients were constrained to a low number but lesion based analysis was supporting, anyway, the conclusions from the present analysis call for further confirmation from larger observations. One would surmise that an analysis of an expanded and more diverse cohort population could have improved the results concerning e.g. the SUV lesion volume dependences. Thus for example, assessing the influence of Body Mass Index (BMI) of larger patients on β-factor optimization remained outside the scope of this study. In addition to that, according to previous studies with 18F-FDG such as Jonmarker et al, BSREM optimazation can depend on the injected dose. Hence, due to the failure to evaluate different

scan durations and injected doses, BSREM performance under aforementioned conditions is unknown. And finally, in PET/CT imaging with 68Ga-PSMA injection, the high absorption in bladder and kidenys compared to surrounding soft tissue caused halo artifacts [24]. In our research, we excluded the effect of this artifact in our evaluations. Therefore, this BSREM analysis warrants further study to ascertain and clarify the diagnostic efficacy for 68Ga-PSMA PET imaging.

Conclusion

In conclusion, BSREM provides an improvement in quantitative accuracy such as SUV_{max}, CR and SNR by a fully convergent image voxel via applying penalization factor to control image noise. In clinical study, increased SNR, SBR and contrast could be attained at similar liver homogeneity compared to OSEM. Differences in quantitative parameters between β-values in small lesions is more considerable than large lesions and the optimal β-value is suggested at 500 for subcentimetric lesions. Also, lesion size had an significant effect on BSREM optimization; as the lesion size decreased, the optimum β-value decreased.

Declarations

Acknowledgments: This work was supported under grant number 52599, Tehran University of Medical Sciences, Tehran, Iran.

Compliance with Ethical Standards:

- **Disclosure of potential conflicts of interest:**

The authors declare that they have no conflict of interest.

- **Research involving human participants and/or animals:**

This article does not contain any studies with human participants or animals performed by any of the authors and is only a retrospective study. The anonymized patient's data were used in this study which approved by Research Ethics Committees of Imam Khomeini Hospital Complex- Tehran University of Medical Sciences (Approval code: IR.TUMS.IKHC.REC.1400.312).

- **Informed consent:**

No informed consent was required due to the anonymized patient's data were used.

References

1. Czernin J, Schelbert H (2004) PET/CT imaging: facts, opinions, hopes, and questions. Journal of Nuclear Medicine 45:1S-3S

2. Messerli M, Stolzmann P, Egger-Sigg M et al (2018) Impact of a Bayesian penalized likelihood reconstruction algorithm on image quality in novel digital PET/CT: clinical implications for the assessment of lung tumors. EJNMMI physics 5:1-13. https://doi.org/10.1186/s40658-018-0223-x
3. Reynés-Llompart G, Gámez-Cenzano C, Vercher-Conejero JL, Sabaté-Llobera A, Calvo-Malvar N, Martí-Climent JM (2018) Phantom, clinical, and texture indices evaluation and optimization of a penalized-likelihood image reconstruction method (Q. Clear) on a BGO PET/CT scanner. Medical physics 45:3214-3222. https://doi.org/10.1002/mp.12986
4. Lantos J, Mittra ES, Levin CS, Iagaru A (2018) Standard OSEM vs. regularized PET image reconstruction: qualitative and quantitative comparison using phantom data and various clinical radiopharmaceuticals. Am J Nucl Med Mol Imaging 8:110
5. Ross S (2014) Q. clear. GE Healthcare, White Paper:1-9
6. Teoh EJ, McGowan DR, Macpherson RE, Bradley KM, Gleeson FV (2015) Phantom and clinical evaluation of the Bayesian penalized likelihood reconstruction algorithm Q. Clear on an LYSO PET/CT system. Journal of Nuclear Medicine 56:1447-1452. https://doi.org/10.2967
7. Liberini V, Messerli M, Husmann L et al (2021) Improved detection of in-transit metastases of malignant melanoma with BSREM reconstruction in digital [18F] FDG PET/CT. European radiology 31:8011-8020. https://doi.org/10.1007/s00330-021-07852-7
8. Caribé PR, Koole M, D'Asseler Y, Van den Broeck B, Vandenberghe S (2019) Noise reduction using a Bayesian penalized-likelihood reconstruction algorithm on a time-of-flight PET-CT scanner. EJNMMI physics 6:1-14. https://doi.org/10.1186/s40658-019-0264-9
9. Sasikumar A (2017) Specificity of 68Ga-PSMA PET/CT for prostate cancer-myths and reality. Indian Journal of Nuclear Medicine: IJNM: the Official Journal of the Society of Nuclear Medicine, India 32:11. https://doi.org/10.4103/0972-3919.198449
10. Jonmarker O, Axelsson R, Nilsson T, Gabrielson S (2021) Comparison of Regularized Reconstruction and Ordered Subset Expectation Maximization Reconstruction in the Diagnostics of Prostate Cancer Using Digital Time-of-Flight 68Ga-PSMA-11 PET/CT Imaging. Diagnostics 11:630. https://doi.org/10.3390/diagnostics11040630
11. Lindström E, Velikyan I, Regula N et al (2019) Regularized reconstruction of digital time-of-flight 68Ga-PSMA-11 PET/CT for the detection of recurrent disease in prostate cancer patients. Theranostics 9:3476. https://doi.org/10.7150/thno.31970
12. Reynés-Llompart G, Gámez-Cenzano C, Romero-Zayas I, Rodríguez-Bel L, Vercher-Conejero JL, Martí-Climent JM (2017) Performance characteristics of the whole-body discovery IQ PET/CT system. Journal of Nuclear Medicine 58:1155-1161. https://doi.org/10.2967/jnumed.116.185561
13. NEMA I (1998) International standard: Radionuclide imaging devices characteristics and test conditions part 1: Positron emission tomographs. International Electrotechnical Commission (IEC), Tech Rep, IEC:61675-61671
14. Association NEM (2001) Performance measurements of positron emission tomographs. NEMA standards publication NU 2-2001

15. Daube-Witherspoon ME, Karp JS, Casey ME et al (2002) PET performance measurements using the NEMA NU 2-2001 standard. Journal of Nuclear Medicine 43:1398-1409
16. Lindström E, Sundin A, Trampal C et al (2018) Evaluation of penalized-likelihood estimation reconstruction on a digital time-of-flight PET/CT scanner for 18F-FDG whole-body examinations. Journal of Nuclear Medicine 59:1152-1158. https://doi.org/10.2967/jnumed.117.200790
17. Liberini V, Pizzuto DA, Messerli M et al (2022) BSREM for Brain Metastasis Detection with 18F-FDG-PET/CT in Lung Cancer Patients. Journal of Digital Imaging 35:581-593. https://doi.org/10.1007/s10278-021-00570-y
18. Lindstrom E, Lindsjo L, Sundin A, Sorensen J, Lubberink M (2020) Evaluation of block-sequential regularized expectation maximization reconstruction of (68) Ga-DOTATOC, F-18-fluoride, and (11) C-acetate whole-body examinations acquired on a digital time-of-flight PET/CT scanner. EJNMMI physics 7. https://doi.org/10.1186/s40658-020-00310-1
19. Ter Voert EE, Muehlematter UJ, Delso G et al (2018) Quantitative performance and optimal regularization parameter in block sequential regularized expectation maximization reconstructions in clinical 68Ga-PSMA PET/MR. EJNMMI research 8:1-15. https://doi.org/10.1186/s13550-018-0414-4
20. Lohaus N, Enderlin F, Skawran S et al (2022) Impact of Bayesian penalized likelihood reconstruction on quantitative and qualitative aspects for pulmonary nodule detection in digital 2-[18F] FDG-PET/CT. Scientific Reports 12:1-10. https://doi.org/10.1038/s41598-022-09904-4
21. Trägårdh E, Minarik D, Almquist H et al (2019) Impact of acquisition time and penalizing factor in a block-sequential regularized expectation maximization reconstruction algorithm on a Si-photomultiplier-based PET-CT system for 18F-FDG. EJNMMI research 9:1-10. https://doi.org/10.1186/s13550-019-0535-4
22. Wang Y, Lin L, Quan W, Li J, Li W (2022) Effect of Bayesian penalty likelihood algorithm on 18F-FDG PET/CT image of lymphoma. Nuclear medicine communications 43:284. https://doi.org/10.1097/MNM.0000000000001516
23. Du J, Ariño-Estrada G, Bai X, Cherry SR (2020) Performance comparison of dual-ended readout depth-encoding PET detectors based on BGO and LYSO crystals. Physics in Medicine & Biology 65:235030. https://doi.org/10.1088/1361-6560/abc365
24. Afshar-Oromieh A, Avtzi E, Giesel FL et al (2015) The diagnostic value of PET/CT imaging with the 68Ga-labelled PSMA ligand HBED-CC in the diagnosis of recurrent prostate cancer. European journal of nuclear medicine and molecular imaging 42:197-209. https://doi.org/10.1007/s00259-014-2949-6

Figures

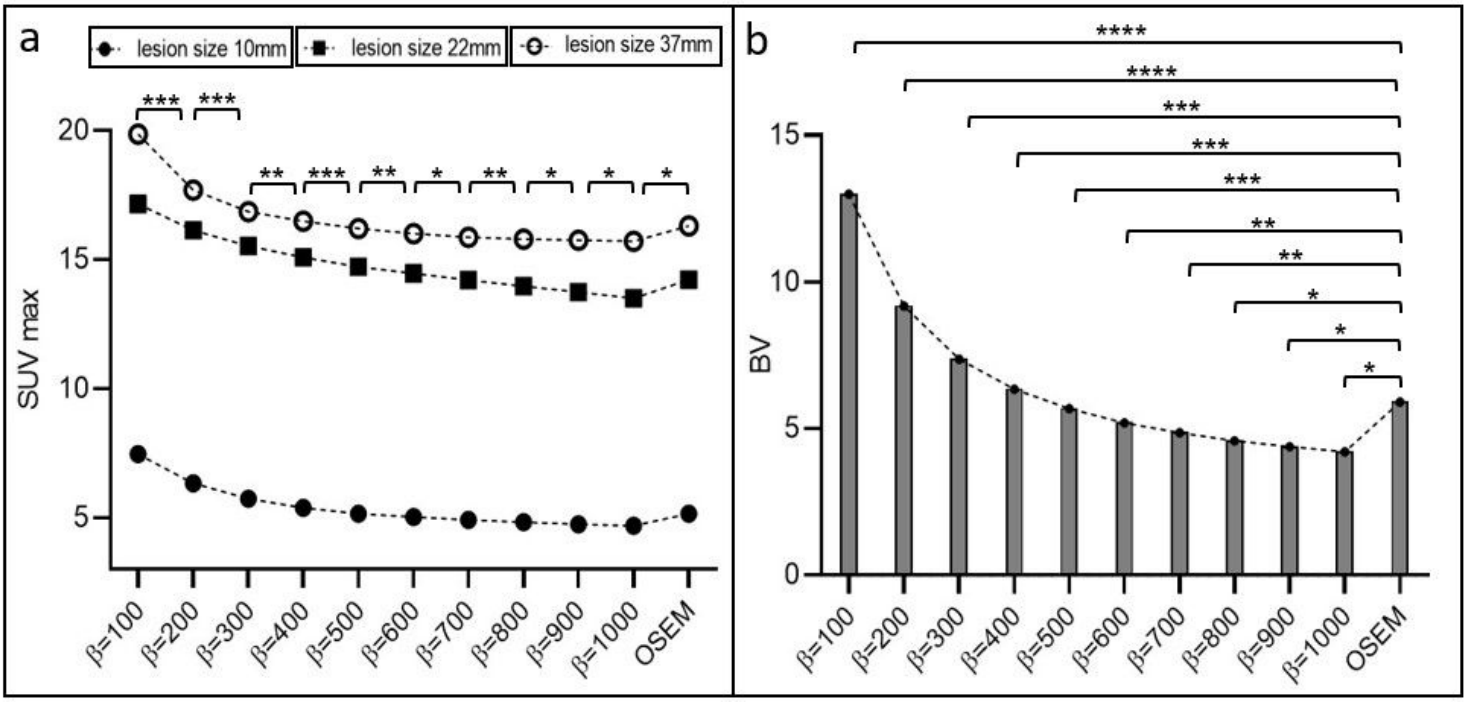

Figure 1

(a) A schematic comparison of 10 mm, 22 mm, and 37 mm hot spheres in SUV_{max} versus different reconstruction methods (with varying BSREM β-values of 100-1000 and OSEM) acquired with a NEMA image quality phantom. (b) Background variability results for BSREM using the same β-values (100-1000) and OSEM reconstruction. Note the asterisk in the figures illustrate the p-value obtained by paired t-test between the two reconstruction methods such that * shows p<0.01, ** (p<0.001), *** (p<0.0001) and **** (p<0.00001).

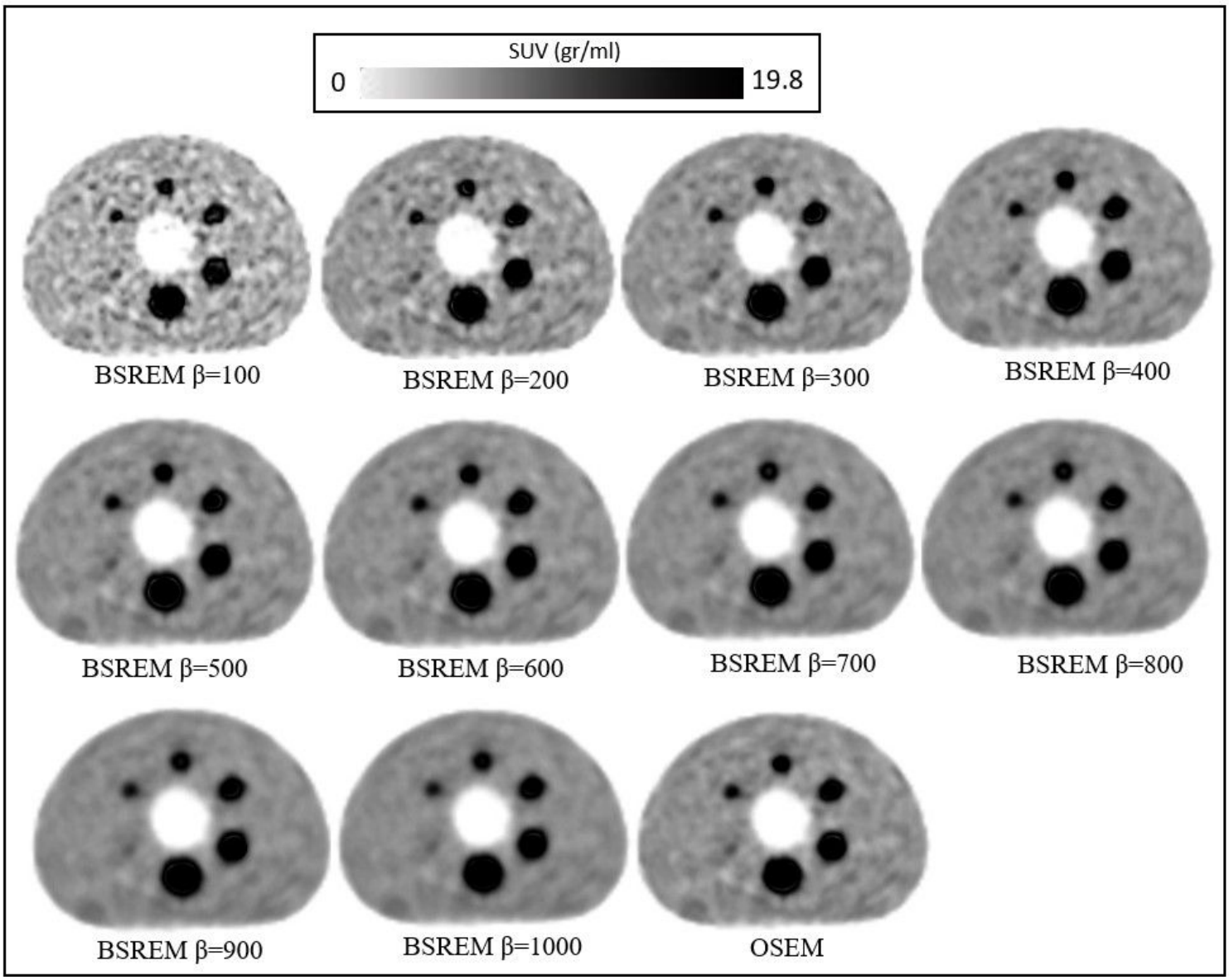

Figure 2

Central transfer slice of NEMA image quality phantom reconstructed by OSEM and BSREM using 25 iterations and β-value 100-1000, at interval of 100. The corresponding OSEM image was reconstructed with 4 iterations, 24 subsets and 4.8 mm post filtering.

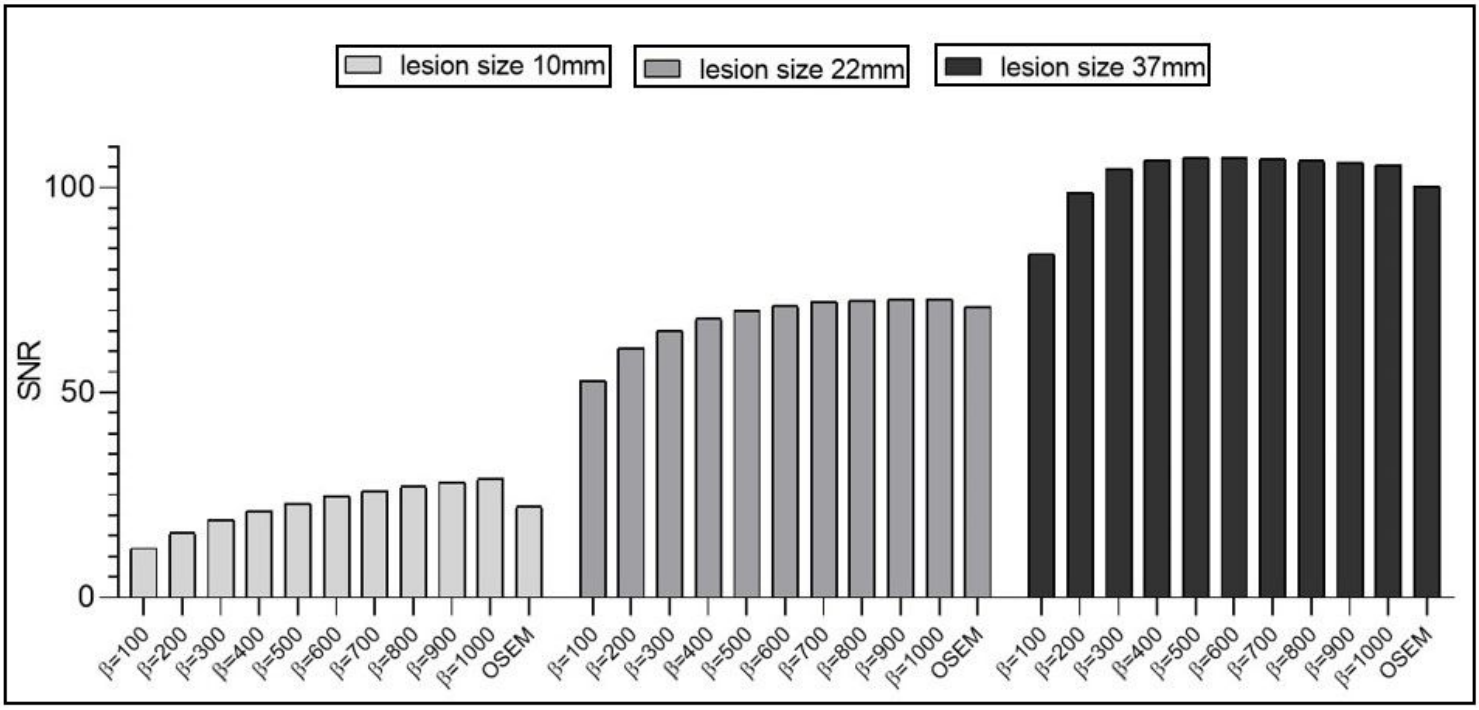

Figure 3

SNR measurment results for 10 mm hot sphere, 22 mm hot sphere and 37 mm hot sphere in NEMA image quality phantom study with different reconstructions: BSREM using β-value in a range between 100 and 1000 and OSEM algorithm.

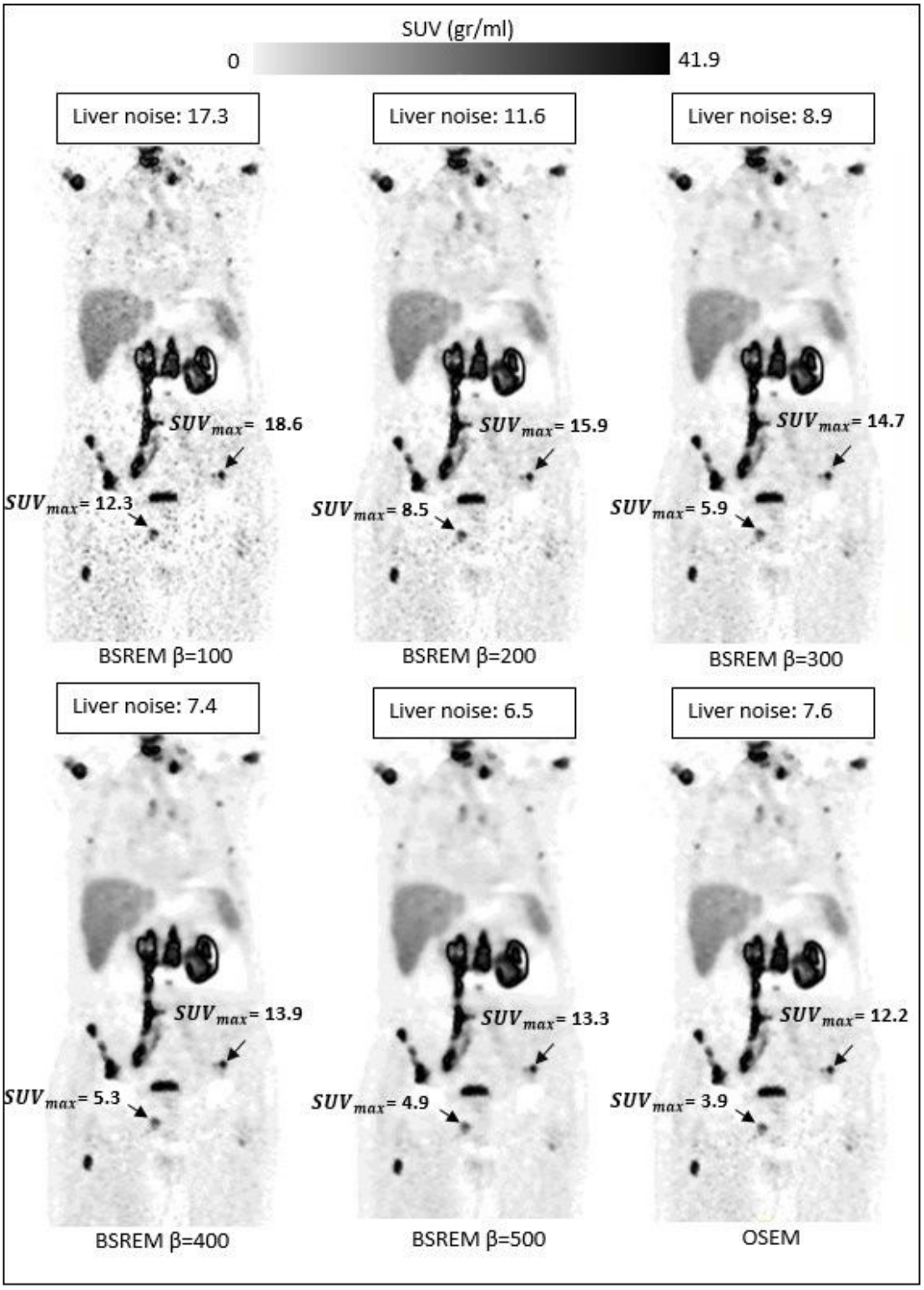

Figure 4

Coronal slice of a prostate cancer patient who underwent 68Ga-PMSA PET/CT examination. Images were reconstructed by OSEM and BSREM. BSREM using 25 iterations and β-value 100-500, at an interval of 100 was used. OSEM reconstruction with 4 iterations, 24 subsets and 4.8 mm post filtering was performed. The SUV_{max} of lesions (arrow) and liver noise is shown for each reconstruction.

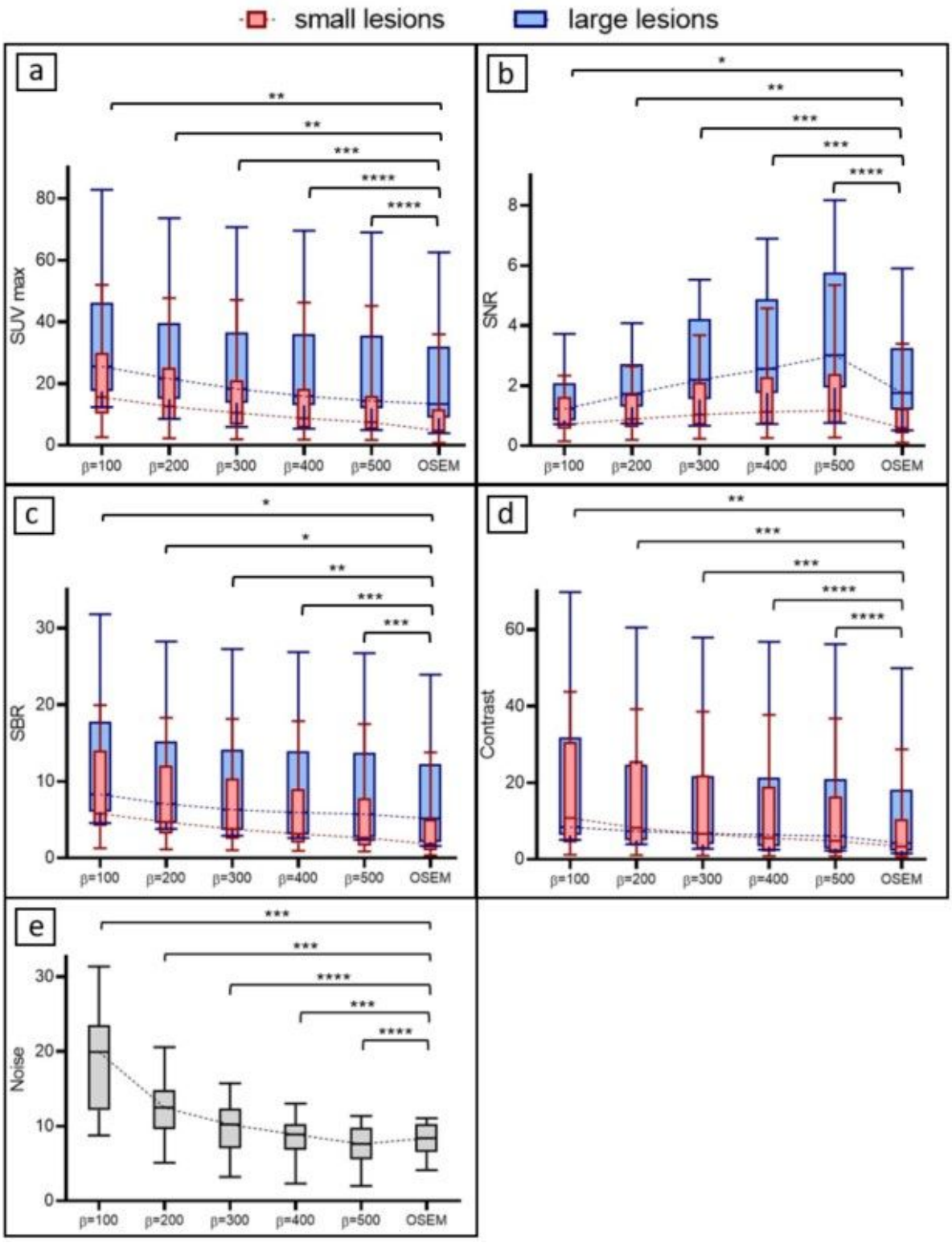

Figure 5

The mean SUV_{max}(a) , SNR (b), SBR (c), contrast (d) for two lesion size groups (small and large) and noise in homogeneous area of liver (e) in clinical study with 68Ga-PSMA. Reconstruction methods employed were OSEM, and BSREM using β-values ranging from 100-500 intervaled atsteps of 100. The dotted lines connect the median values. Note the asterisks in the diagrams illustrate the p-values

obtained by paired t-test between the two reconstruction methods with * depicting $p<0.01$, ** showing $p<0.001$, *** for $p<0.0001$ and **** for $p<0.00001$.